Enhanced ability of information gathering may intensify disagreement among groups

Hiroki Sayama*
Center for Collective Dynamics of Complex Systems, Binghamton University, Binghamton, NY 13902-6000, USA
Max Planck Institute for the Physics of Complex Systems, 01187 Dresden, Germany and
Waseda Innovation Lab, Waseda University, Shinjuku, Tokyo 169-8050, Japan
(Dated: October 29, 2021)

Today's society faces widening disagreement and conflicts among constituents with incompatible views. Escalated views and opinions are seen not only in radical ideology or extremism but also in many other scenes of our everyday life. Here we show that widening disagreement among groups may be linked to the advancement of information communication technology, by analyzing a mathematical model of population dynamics in a continuous opinion space. We adopted the interaction kernel approach to model enhancement of people's information gathering ability and introduced a generalized non-local gradient as individuals' perception kernel. We found that the characteristic distance between population peaks becomes greater as the wider range of opinions becomes available to individuals or the greater attention is attracted to opinions distant from theirs. These findings may provide a possible explanation for why disagreement is growing in today's increasingly interconnected society, without attributing its cause only to specific individuals or events.

arXiv:2002.01049v2 [physics.soc-ph] 15 Jun 2020

I. INTRODUCTION

Today's society faces many urgent critical challenges. One of such challenges is addressing the widening disagreement and conflicts among different social constituent groups with incompatible views on politics, economy, international relationships, religions, cultures, lifestyle, and other aspects of our life.

Studies on this challenge often focus on how escalated views and opinions emerge in society [1]. Typical approaches in this area include detection of extremism in online media [2–4] and modeling contagious processes of extremism through social networks [5, 6]. While highly relevant to and valuable for national security concerns, these approaches necessarily impose an asymmetric point of view to consider one side as the cause of the problem ("us" being normal vs. "them" being abnormal), making it difficult to obtain a more system-oriented understanding of how such conflicts may arise and widen spontaneously at a global societal scale.

Escalated views and opinions are seen not only in radical ideology or extremism, but also in many other scenes of our everyday life (typically in a milder form), such as political conversations in social media [7, 8], healthcare choices (e.g., anti-vax movement) [9, 10], and dietary preferences [11, 12], to name a few. The widening disagreement among those who have escalated views is becoming more prevalent than before on a variety of subjects. Part of the cause is often suspected to be the recent advances of information communication technology (e.g., web media, social media, smart phones, and other forms of high-speed, high-volume, personalized communication)[9, 13–15] that continuously increase information gathering intensity and enhance users ability to choose their preferred information sources (with some caveats [16]). In this view, widening disagreement may be modeled and understood as a spontaneous pattern formation process in which people's information gathering ability plays a key role as the control parameter. The present study explores this view through mathematical modeling and analysis of opinion dynamics.

In this study, we combine the opinion dynamics with spatial models studied in mathematical biology. Specifically, we describe the dynamics of popularities of a wide range of opinions in partial differential equations (PDEs), inspired by models of diffusion and migration of biological organisms [17, 18]. In particular, we adopt a model of auto-aggregation [19–22] in which organisms aggregate together through a hill-climbing migration behavior on a terrain of signals. In our case, we consider people migrating in a space of opinions, and their migration is driven by the gradient of the opinion popularity itself.

We also propose a principled way to generalize local gradient into non-local perceived gradient based on the interaction kernel approach used in physics, applied mathematics, and mathematical biology. This allows us to model the enhancement of people's information gathering ability, which would not be captured by simply using a conventional local gradient at a single point in the opinion space. It also allows for parametrization of two distinct aspects of non-local perception: the breadth of information gathering and the level of selective attention paid to distant opinions, the latter of which we hypothesize to play a particularly significant role in social opinion drift [23, 24]. The model and the results of our analytical and numerical investigations are reported below.

II. MODEL

Our mathematical model represents the dynamics of popularities of opinions using a population distribution

* sayama@binghamton.edu; http://bingweb.binghamton.edu/~sayama/

function $P(x,t)$ for opinion x and time $t \geq 0$ (Fig. 1a, top). $P(x,t)$ is the number (in an arbitrary unit) of people whose current opinion is x at time t. We assume the population never grows or decays, so the only changes possible in this model are due to diffusion and migration. Diffusion represents random fluctuations of people's opinions, while migration represents directed, active change of people's opinions caused by social influence. More specifically, we adopt a widely used assumption [25–27] that people will more likely adopt opinions that are more supported by others. We also assume the homophily principle [14, 28, 29] in people's information gathering behavior, which implies that they perceive information only from a vicinity of their own opinion in the opinion space. The last two assumptions simplify the migration process into a simple hill-climbing behavior following the gradient of $P(x,t)$. Note that the opinion space modeled here is different from physical space within which individuals exchange opinions (e.g., social networks). Such social structure is not modeled explicitly in this study.

Both diffusion and migration can be modeled using the transport equation framework [18, 22, 30]. The model equation we use in this study to describe the dynamics of $P(x,t)$ is

$$\frac{\partial P}{\partial t} = d\nabla^2 P - c\nabla \cdot (PG(P)), \tag{1}$$

where $d\nabla^2 P$ is the diffusion term and $-c\nabla \cdot (PG(P))$ is the migration term. $G(P)$ is the *perceived* gradient of popularity distribution, defined as

$$G(P) = \int_{-\infty}^{\infty} P(x+y,t)g(y)dy, \tag{2}$$

$$g(y) = \frac{1}{2\mu} \cdot \frac{1}{\sqrt{2\pi}\sigma} \left(e^{-\frac{1}{2}\left(\frac{y-\mu}{\sigma}\right)^2} - e^{-\frac{1}{2}\left(\frac{y+\mu}{\sigma}\right)^2} \right). \tag{3}$$

Eq. (2) shows that the perceived gradient is defined as a cross-correlation between P and a perception kernel g given in Eq. (3) (Fig. 1a, bottom), based on the interaction kernel approach commonly used in physics, applied mathematics, and mathematical biology [21, 30, 31]. The perception kernel g describes how people assign weights (attentions) to nearby opinions' popularities when they assess the gradient. In this study, we define the perception kernel as a combination of two Gaussian distributions whose width is determined by σ and whose means are separated by 2μ across the origin, one positive on the right hand side and one negative on the left hand side, to capture the difference of popularity levels between the two sides (Fig. 1b).

Note that $G(P)$ converges to a simple derivative $P'(x)$ in the limit of $\mu \to 0^+$ and $\sigma \to 0^+$, i.e., when g is made of two Dirac's delta functions positioned right next to the origin with opposite signs (see Appendix A). This indicates that $G(P)$ can be considered a mathematically valid non-local generalization of a spatial derivative.

This generalization of the gradient enables us to explore different shapes of the perception kernel by varying σ and μ (Fig. 1c) and study their effects on opinion dynamics, which would not have been possible if only local gradient were used. For example, increasing σ (Fig. 1c, bottom left) represents a situation in which people can gather information from a broader range of opinions. Meanwhile, increasing μ (Fig. 1c, top right) represents a situation in which people tend to pay great attention particularly to distant, extreme opinions, which may correspond to sensationalism widely practiced in various media today.

III. RESULTS

A. Stability analysis

We first conduct linear stability analysis of Eq. (1) to find the conditions under which homogeneous population distributions are unstable and thus heterogeneous patterns will form. We begin the analysis by replacing the spatio-temporal function $P(x,t)$ with a constant homogeneous population level P_h plus a sinusoidal spatial perturbation with temporally changing small amplitude $\Delta P(t)$ [18], as follows:

$$P(x,t) \to P_h + \Delta P(t)\sin(\omega x + \phi) \tag{4}$$

This replacement allows for linearization of Eq. (1) into the following non-spatial linear dynamical equation of ΔP (see Appendix B for details):

$$\frac{d\Delta P}{dt} = \left(-d\omega^2 + c\omega P_h \int_{-\infty}^{\infty} \sin(\omega y)g(y)dy \right) \Delta P \tag{5}$$

Therefore, with $Q(\omega) = \int_{-\infty}^{\infty} \frac{\sin(\omega y)}{\omega} g(y)dy$, if

$$Q(\omega) > \frac{d}{cP_h} \tag{6}$$

for $\omega > 0$, then the homogeneous population distribution is unstable and a non-homogeneous pattern (i.e., islands of popular opinions = distinct groups) will form in the opinion space. This result already tells us that groups are more likely to form if (1) diffusion is weaker, (2) active migration is stronger, and/or (3) the population level is greater. These findings are consistent with results obtained for other similar auto-aggregation models [17–20].

We also note that the range of $Q(\omega)$ is bounded to $[-1,1]$ and $Q(\omega)$ approaches its maximum 1 as $\omega \to 0$ regardless of the shape of the perception kernel (see Appendix C). Therefore, in a sufficiently large opinion space, the low-frequency perturbations always destabilize the homogeneous distribution eventually if and only if

$$1 > \frac{d}{cP_h}, \quad \text{or} \quad cP_h > d. \tag{7}$$

which was also confirmed through numerical simulations (see Appendix D).

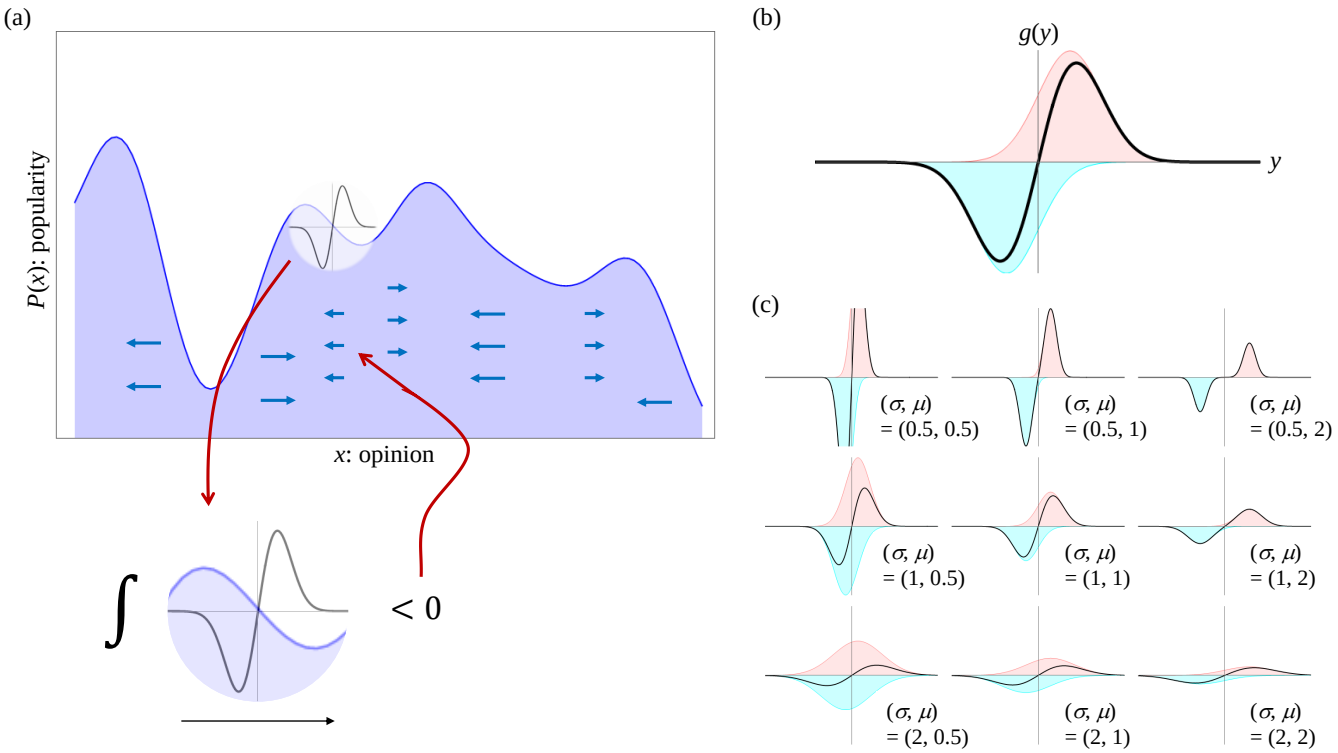


FIG. 1. Schematic overview of the mathematical model proposed in this study. (a) Popularities of opinions represented as distribution $P(x,t)$ on opinion x. $P(x,t)$ follows diffusion-migration dynamics described in Eq. (1), which may show, under typical parameter settings, aggregation behaviors as illustrated by small horizontal arrows in this figure. Directions of migrations are determined by a perceived gradient $G(P)$ defined as a cross-correlation between $P(x,t)$ and a perception kernel $g(y)$ at each location x (Eq. (2), also depicted at the bottom of this panel). (b) Structure of the perception kernel $g(y)$ (Eq. (3)). The black solid curve shows the shape of $g(y)$, which is the sum of two Gaussian distributions with opposite signs (pink and cyan), one placed on the right and another on the left. (c) Variations of shapes of $g(y)$ as σ and μ are varied. Having sharp peaks near the center in $g(y)$ (top left) makes $G(P)$ close to a conventional local derivative, corresponding to the case in which individuals' attention is limited only to opinions of similarly minded others. Having broader and/or distant peaks means enhanced information gathering ability, covering a wider range of opinions and/or paying greater attention to distant opinions, respectively.

B. Numerical study on the disagreement between groups

Our main interest in this study is in the characteristic value of ω for instability. This is because the spatial period of perturbation, $L = 2\pi/\omega$, determines how far away the islands of opinions are separated from each other in the opinion space, which indicates the extent of disagreement between groups.

We numerically calculated the values of $Q(\omega)$ while varying σ and μ. Results are shown in Fig. 2, in which warmer colors indicate spatial frequencies ω that are more likely to destabilize the homogeneous population distribution (depending on the value of $\frac{d}{cP_h}$ as discussed above). These plots show that, the greater σ and/or μ are, the more concentrated on low-frequency regions the unstable perturbations are, which correspond to greater distances between spontaneously formed groups.

Figure 3 shows actual numerical simulation results in a space-time plot for several values of σ and μ. Periodic boundary condition was used to avoid potential artifacts arising from cut-off spatial boundaries [32]. The population distribution initially remain more or less homogeneous for a certain period of time, but then distinct peaks (groups) quickly form. Once established, those groups become stable and remain unchanged for a substantially long period of time. Interestingly, the intervals between those peaks are longer for greater values of σ and/or μ, which can be interpreted in that the disagreement among those established groups becomes more intense as people's information gathering ability is enhanced. It is also noticeable that the effects of σ and μ are slightly different on the group formation process.

Figure 4 summarizes these results in a single plot of the characteristic inter-peak distance L as a function of σ and μ for $P_h = 1$, $c = 1$ and $d = 0.2$. The surface plot shows a numerically obtained lower bound of L based on the analysis (Eq. (6)). Our analysis predicts that perturbations with a characteristic length below this surface would not grow. The peak distances obtained from nu-

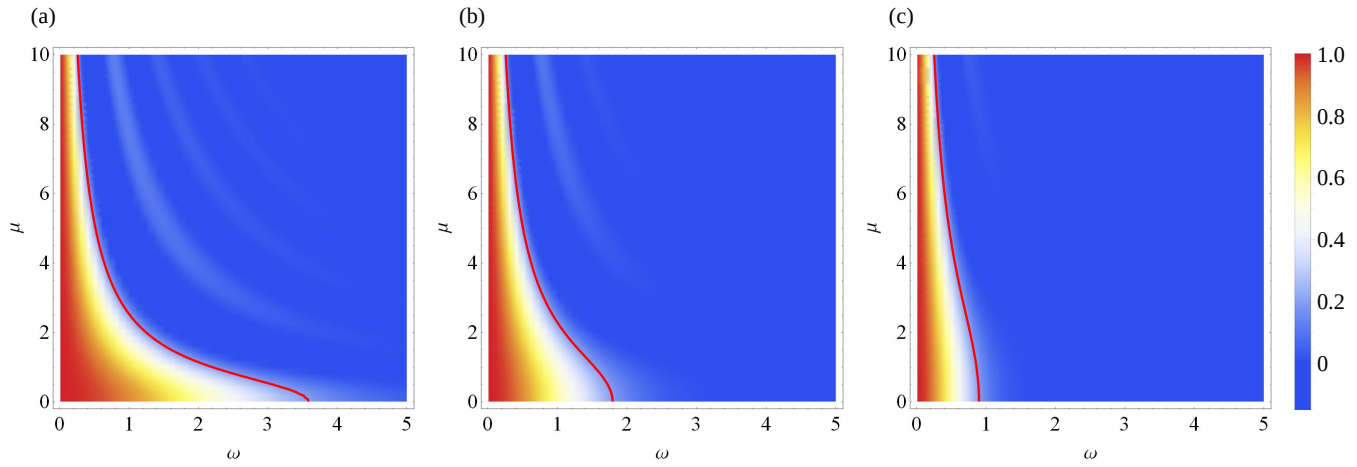


FIG. 2. Heatmaps showing the value of $Q(\omega)$ as a function of ω (horizontal axis), μ (vertical axis) and σ (varied in three panels; (a) $\sigma = 0.5$, (b) $\sigma = 1$, (c) $\sigma = 2$). Red curves show contours that correspond to $Q(\omega) = \frac{d}{cP_h} = 0.2$, the critical threshold under the parameter setting used for numerical simulations in this paper.

merical simulations (blue dots in Fig. 4) are all above this surface, which confirms that our analysis was valid. It is seen in the figure that the characteristic inter-peak distance grows almost linearly with σ and μ, with a mild nonlinear interaction between them.

C. Temporal change of information gathering ability

This model allows us to test more dynamic scenarios in which people's information gathering ability changes over time. Investigation of such hypothetical scenarios can provide us with valuable insight on potential interventions and possible societal responses to them. We test two hypothetical dynamic scenarios below.

The first scenario assumes that people's information gathering ability gradually increases over time. This can be simulated by increasing values of σ and μ in the course of a numerical simulation. This scenario imitates gradual advancement of information communication technology, by which people gain access to a broader range of opinions (by greater σ) and pay greater attention to opinions distant from their own (by greater μ). Figure 5a shows an illustrative example of this scenario, in which both σ and μ, initially set to 0.5, begin to increase linearly with time at $t = 20$, up to 5.0 by the end of the simulation at $t = 200$. The smaller groups existing at the beginning gradually merge to form larger, more distant (more disagreeing) groups as σ and μ increase. By the end of this particular simulation, more than a dozen of initial small groups are integrated into just three large groups.

The second scenario models an attempt of external intervention to the population behavior observed in the first scenario. Specifically, we test what would happen if people's information gathering ability were suppressed in the middle of the first scenario with an intention to dissolve the emerging larger groups. This scenario can be considered a simulation of government regulation or other forms of exogenous control, which can be simulated by lowering the values of σ and μ after a certain period of group formation. Figure 5b shows an example of this scenario, which proceeds the exact same way as in Fig. 5a for the first half but then σ and μ are suddenly reset to their initial value 0.5 at $t = 100$ and remain constant thereafter. Interestingly, the large groups that are already established by the time of the intervention never become diffused, but to the contrary, they become more concentrated and more stable than before the intervention. This is because, unlike in other spatial biological/ecological models that have parameter-dependent characteristic scales of patterns [33–36], groups are generally stable in auto-aggregation models like ours once they are established, regardless of parameter values of aggregation behavior. They may be absorbed into other groups or destroyed by sufficiently strong diffusion, but it is extremely difficult for them to disintegrate into smaller groups. This result implies that suppressing people's information gathering may not work as a means to dissolve those large groups with conflicting opinions, if they are already established.

IV. DISCUSSIONS AND CONCLUSIONS

In this study, we proposed a PDE-based mathematical model of opinion dynamics in a continuous opinion space and studied its dynamics using both analytical and numerical means. Contributions of this work can be summarized in the following four points.

First, we presented an unconventional perspective to consider growing disagreement and conflicts in society the result of spontaneous pattern formation in an opinion space, in which the characteristic distance between

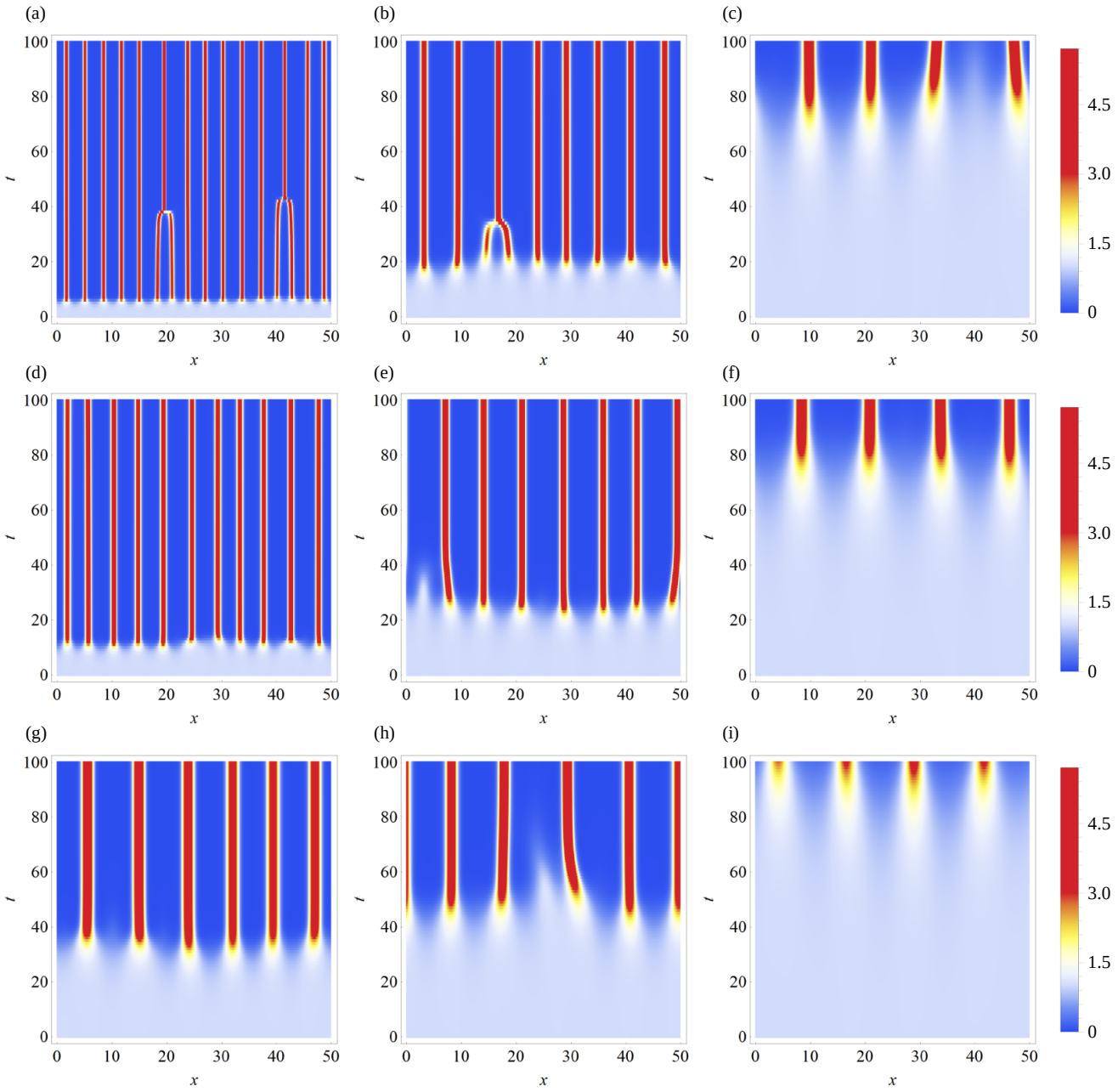


FIG. 3. Numerical simulation results of the population dynamics of the proposed model visualized in space (x: horizontal axis) and time (t: vertical axis, going from bottom to top). Colors represent population density (blue = 0, cold = low, warm = high, red = 3 or above). $P_h = 1$, $c = 1$, and $d = 0.2$. See the Methods section for details of numerical integration. Results with several different values of σ and μ are shown in this figure (left column (a, d, g): $\sigma = 0.5$, center column (b, e, h): $\sigma = 1.0$, right column (c, f, i): $\sigma = 2.0$; top row (a, b, c): $\mu = 0.5$, middle row (d, e, f): $\mu = 1.0$, bottom row (g, h, i): $\mu = 2.0$). The average distance L between population peaks at $t = 100$ was as follows: (a) $((\sigma, \mu) = (0.5, 0.5))$: $L = 3.57143$; (b) $((\sigma, \mu) = (1.0, 0.5))$: $L = 6.25$; (c) $((\sigma, \mu) = (2.0, 0.5))$: $L = 12.5$; (d) $((\sigma, \mu) = (0.5, 1.0))$: $L = 4.54545$; (e) $((\sigma, \mu) = (1.0, 1.0))$: $L = 7.14286$; (f) $((\sigma, \mu) = (2.0, 1.0))$: $L = 12.5$; (g) $((\sigma, \mu) = (0.5, 2.0))$: $L = 8.33333$; (h) $((\sigma, \mu) = (1.0, 2.0))$: $L = 10.$; (i) $((\sigma, \mu) = (2.0, 2.0))$: $L = 12.5$.

population peaks represents how severe the disagreement is among distinct groups. This perspective allows us to understand intensifying disagreement as a system-level global property rather than a consequence caused by specific individuals or events to blame. Second, we proposed a generalized non-local spatial gradient and used it as a mathematical representation of enhanced information gathering ability of people. This enabled us to explore different shapes of perception kernels and also facilitated the linear stability analysis of the model. Third,

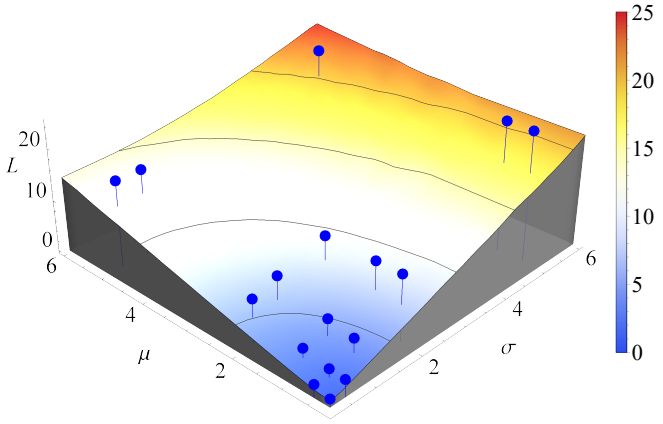


FIG. 4. Characteristic distance between population peaks (L) visualized as a function of σ and μ. $P_h = 1$, $c = 1$, $d = 0.2$. The surface plot shows a critical lower bound L_c below which such perturbations would not grow. The lower bound L_c was obtained as $L_c = \frac{2\pi}{\omega_c}$, where ω_c is a numerically obtained critical value of ω that satisfies $Q(\omega) = \frac{d}{cP_h}$. The blue dots show actual peak distances measured in numerical simulations (e.g., Fig. 3), which are all above the surface. This confirms the validity of the analytical prediction that enhanced information gathering ability (increased σ and/or μ) always results in greater distance between population peaks.

we obtained several key analytical results on the general threshold between pattern-forming and non-pattern-forming regimes, as well as the effects of the parameters of information gathering behavior on the distance between resulting groups, which were confirmed by numerical simulations. The result clearly showed that the distance among groups became greater as people's information gathering ability was enhanced. Finally, we tested a few dynamic scenarios that produced relevant implications of increasing information communication technology for social dynamics and also some insight into the (lack of) effectiveness of external interventions.

Our results are generally in agreement with the now commonly made claim that the rapid development of the Internet, social media, smart phones, and other personal information communication technologies have contributed to the increase of societal conflicts and ideological escalation. Our information gathering ability today is nothing comparable even to that of twenty years ago, and such a rapid change of our "perception kernel" may have already been producing emergent macroscopic social patterns (like those shown in Fig. 5) that go beyond any single individual's intention.

The results of the last scenario simulations illustrate challenging aspects of the observed opinion dynamics. As the perception kernel becomes wider and/or more focused on distant opinions, groups tend to merge hierarchically to eventually form a small number of large groups that are in significant disagreement from each other. Once they have formed, reducing the perception kernel would have no effect on their existence, but rather, it helps those groups more crystallized. This leads us to questioning whether there are ways to remedy disagreement between those large groups and let them gracefully revert back to smaller groups with more distributed, more diversified opinions.

Our model suggests that, at least mathematically, several different options exist for addressing this question. The first option is to increase the random diffusion rate d or decrease the active migration rate c so that Eq. (6) no longer holds. The second option is to reduce μ all the way to a negative value so that people seek originality rather than social conformity, changing the dynamics of the model from auto aggregation to auto avoidance. These two options are essentially suggesting to alter people's behavior, but it is not obvious how one could achieve such global behavioral changes in reality (some well-designed educational initiatives might help). The third option is to increase σ and μ to extremely large values so that the boundaries of groups become more gradual and less defined (a sign of this phenomenon is seen near the end of the simulation in Fig. 5a). The last option suggests to *promote*, rather than suppress, people's information gathering, but it would then bring another problem that people's cognitive ability would be too limited to process the massive amount of information collected. None of these options is problem-free, but they may still suggest directions of potential solutions to be explored further.

We conclude this paper by pointing out several limitations of the study and identify future research questions. The model discussed in this study is still quite limited in both mathematical and practical aspects. Mathematically, we used only one form of the perception kernel to facilitate parameterized representation of information gathering behavior, but there should be many other functional forms that are plausible as a model of human information gathering behaviors. For example, it was recently reported that exposure to distant opinions may have a repulsion effect [15], which was not considered in the present study but could be incorporated by revising the shape and sign of the perception kernel. Exploring different forms of the perception kernel and studying their effects on the resulting opinion dynamics would likely produce more comprehensive understanding of this model. We also used only one boundary condition (periodic) in all of the numerical simulations presented, but the interactions of self-organizing patterns with nontrivial boundaries (i.e., structure of possibilities in the idea space) are another area that warrants further systematic study.

In terms of practical aspects, it is with no doubt that our model oversimplified the complexity of real human social dynamics. We assumed only one-dimensional continuous opinion space, but opinions and ideas can be

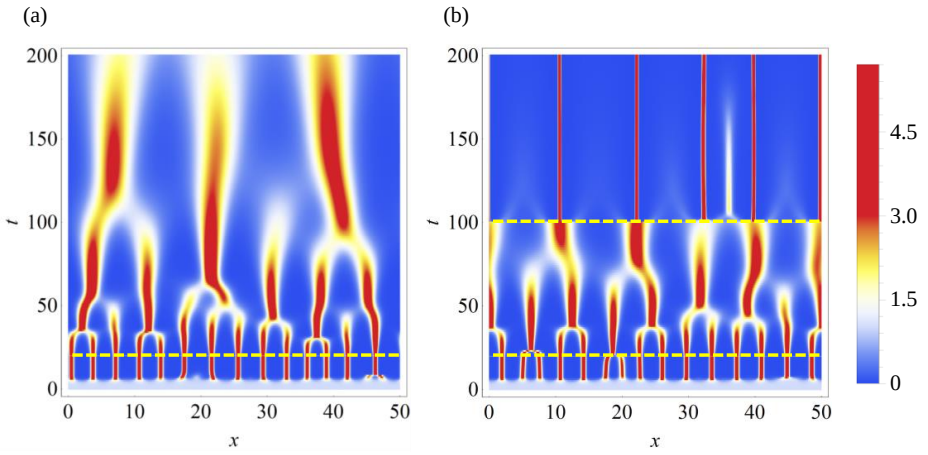


FIG. 5. Numerical simulation results of dynamic scenarios in which the values of σ and μ are varied over time. The simulation method, initial condition, and meaning of colors are all the same as in Fig. 3. Simulations were conducted until $t = 200$ in these plots. Yellow dashed lines represent key time points. (a) Initially $\sigma = \mu = 0.5$, but after $t = 20$ those parameters are linearly increased with time up to 5.0 by $t = 200$. This scenario imitates gradual advance of information communication technology. As σ and μ increase, existing groups tend to merge to form larger, more distant (= disagreeing) groups over time. (b) Conditions are the same as in (a), except that σ and μ are reset to their initial value 0.5 at $t = 100$ and remain constant thereafter. This scenario imitates external intervention to reduce people's information gathering ability, but it fails to diffuse the already established groups.

multi-dimensional. While we expect that the essential conclusions obtained from the stability analysis would still hold in multidimensional opinion space, details of implications would likely be influenced by the number of dimensions. In addition, this study did not explicitly consider non-trivial social network structure of opinion exchange. The structure of society is implicit in this model, represented indirectly by the perception kernel (which allows individuals whose opinion states are close to each other to interact). In other words, the proposed model assumes that social connectivity is dynamically correlated with the proximity of opinions of individuals in the opinion space. Assumptions of nontrivial social network structure with features such as heterogeneous degrees and communities are orthogonal to opinion dynamics, which can be incorporated into the model but is beyond the scope of the present study.

Furthermore, this study did not consider behavioral diversity of individuals within the population at all. Such an assumption of homogeneous attributes shared among all components is still a common practice used in many theoretical studies of social dynamics, yet we have recently shown in a separate study that having even a simplest kind of individual diversity can greatly influence macroscopic behaviors of social systems [37]. Introducing behavioral diversity to the model may produce fundamentally different outcomes and implications. Finally, the proposed model has yet to be validated in comparison with quantitative real-world data. Eq. (7) showed a unique dimensionless quantity $\frac{d}{cP_h}$ and its critical threshold 1. This would allow at least for empirical testing of the global pattern formation condition using real-world data, regardless of specific choices of measurement units. Meanwhile, it might be difficult to obtain a large-scale socio-behavioral data that could be directly used to test the effects of the perception kernel's shape, and therefore, we anticipate the full model validation to be done through multiple hypothesis generation and testing.

METHODS

Numerical integration of the PDEs was conducted in a discretized space-time with spatial interval $\Delta x = 0.05$ and temporal interval $\Delta t = 0.001$ using a simple Euler-forward numerical integration method. The initial condition was a homogeneous population at $P_h = 1$ everywhere in a spatial domain $[0, 50]$, with small random perturbation (a random number sampled from a uniform distribution $[-0.02, 0.02]$) added to each discrete spatial location. The boundary condition was set to be periodic.

The numerical solver was implemented by the author in Julia 1.3.0, whose source code is available upon request. Analysis and visualization of the simulation results were conducted using Wolfram Research Mathematica 12.0.0.

ACKNOWLEDGMENTS

This work was supported by JSPS KAKENHI Grant Number 19K21571 and the Visitors Program of the Max Planck Institute for the Physics of Complex Systems.

H.S. designed the research, developed the model, conducted mathematical analysis, wrote computer simula-

tion codes, conducted numerical experiments, analyzed the results, and wrote the manuscript.

The author does not have any competing interests.

All correspondence related to this study should be addressed to H.S. (sayama@binghamton.edu).

The data that support the findings of this study (source codes for numerical simulations, mathematical analysis, and visualization, as well as raw data for figures) are available from the author upon request.

[1] Yao-Li Chuang and Maria R D'Orsogna. Mathematical models of radicalization and terrorism. *arXiv preprint arXiv:1903.08485*, 2019.

[2] Emilio Ferrara, Wen-Qiang Wang, Onur Varol, Alessandro Flammini, and Aram Galstyan. Predicting online extremism, content adopters, and interaction reciprocity. In *International Conference on Social Informatics*, pages 22–39. Springer, 2016.

[3] Adam Badawy and Emilio Ferrara. The rise of jihadist propaganda on social networks. *Journal of Computational Social Science*, 1(2):453–470, 2018.

[4] Pedro D Manrique, Minzhang Zheng, Zhenfeng Cao, Elvira Maria Restrepo, and Neil F Johnson. Generalized gelation theory describes onset of online extremist support. *Physical Review Letters*, 121(4):048301, 2018.

[5] John M Berger. The metronome of apocalyptic time: Social media as carrier wave for millenarian contagion. *Perspectives on Terrorism*, 9(4):61–71, 2015.

[6] Emilio Ferrara. Contagion dynamics of extremist propaganda in social networks. *Information Sciences*, 418:1–12, 2017.

[7] Michael D Conover, Jacob Ratkiewicz, Matthew Francisco, Bruno Gonçalves, Filippo Menczer, and Alessandro Flammini. Political polarization on Twitter. In *Fifth International AAAI Conference on Weblogs and Social Media*, 2011.

[8] AJ Morales, Javier Borondo, Juan Carlos Losada, and Rosa M Benito. Measuring political polarization: Twitter shows the two sides of Venezuela. *Chaos: An Interdisciplinary Journal of Nonlinear Science*, 25(3):033114, 2015.

[9] Anna Kata. Anti-vaccine activists, Web 2.0, and the postmodern paradigm–an overview of tactics and tropes used online by the anti-vaccination movement. *Vaccine*, 30(25):3778–3789, 2012.

[10] NF Johnson, N Velasquez, N Johnson Restrepo, R Leahy, N Gabriel, S Wuchty, and D Broniatowski. Health wars and beyond: The rapidly expanding and efficient network insurgency interlinking local and global online crowds of distrust. *arXiv preprint arXiv:1910.02103*, 2019.

[11] Matthew Cole and Karen Morgan. Vegaphobia: derogatory discourses of veganism and the reproduction of speciesism in UK national newspapers. *The British Journal of Sociology*, 62(1):134–153, 2011.

[12] Norelle R Reilly. The gluten-free diet: recognizing fact, fiction, and fad. *The Journal of pediatrics*, 175:206–210, 2016.

[13] Markus Prior. Media and political polarization. *Annual Review of Political Science*, 16:101–127, 2013.

[14] Eytan Bakshy, Solomon Messing, and Lada A Adamic. Exposure to ideologically diverse news and opinion on Facebook. *Science*, 348(6239):1130–1132, 2015.

[15] Christopher A Bail, Lisa P Argyle, Taylor W Brown, John P Bumpus, Haohan Chen, MB Fallin Hunzaker, Jaemin Lee, Marcus Mann, Friedolin Merhout, and Alexander Volfovsky. Exposure to opposing views on social media can increase political polarization. *Proceedings of the National Academy of Sciences*, 115(37):9216–9221, 2018.

[16] Levi Boxell, Matthew Gentzkow, and Jesse M Shapiro. Greater Internet use is not associated with faster growth in political polarization among US demographic groups. *Proceedings of the National Academy of Sciences*, 114(40):10612–10617, 2017.

[17] Leah Edelstein-Keshet. *Mathematical Models in Biology*. SIAM, 2005.

[18] Hiroki Sayama. *Introduction to the Modeling and Analysis of Complex Systems*. Open SUNY Textbooks, 2015.

[19] Evelyn F Keller and Lee A Segel. Initiation of slime mold aggregation viewed as an instability. *Journal of Theoretical Biology*, 26(3):399–415, 1970.

[20] Dirk Horstmann. From 1970 until present: the Keller-Segel model in chemotaxis and its consequences. *Max Planck Institute for Mathematics in the Sciences Preprint*, 3/2003, `https://www.mis.mpg.de/publications/preprints/2003/prepr2003-3.html`, 2003.

[21] Silvia Boi, Vincenzo Capasso, and Daniela Morale. Modeling the aggregative behavior of ants of the species Polyergus rufescens. *Nonlinear Analysis: Real World Applications*, 1(1):163–176, 2000.

[22] Thomas Hillen and Kevin J Painter. A user's guide to PDE models for chemotaxis. *Journal of Mathematical Biology*, 58(1-2):183, 2009.

[23] Hiroki Sayama and Roberta Sinatra. Social diffusion and global drift on networks. *Physical Review E*, 91(3):032809, 2015.

[24] Hiroki Sayama. Going extreme without leaders. `https://medium.com/@hsayama/going-extreme-without-leaders-e2f1ea0ba520`, 2016. Accessed: 2020-01-06.

[25] Morris H DeGroot. Reaching a consensus. *Journal of the American Statistical Association*, 69(345):118–121, 1974.

[26] Noah E Friedkin and Eugene C Johnsen. Social influence and opinions. *Journal of Mathematical Sociology*, 15(3-4):193–206, 1990.

[27] Sven Banisch and Eckehard Olbrich. Opinion polarization by learning from social feedback. *Journal of Mathematical Sociology*, 43(2):76–103, 2019.

[28] Miller McPherson, Lynn Smith-Lovin, and James M Cook. Birds of a feather: Homophily in social networks. *Annual Review of Sociology*, 27(1):415–444, 2001.

[29] Gueorgi Kossinets and Duncan J Watts. Origins of homophily in an evolving social network. *American Journal of Sociology*, 115(2):405–450, 2009.

[30] Marco Di Francesco and Simone Fagioli. Measure solutions for non-local interaction PDEs with two species. *Nonlinearity*, 26(10):2777, 2013.

[31] Alexander Mogilner and Leah Edelstein-Keshet. A non-local model for a swarm. *Journal of Mathematical Biology*, 38(6):534–570, 1999.

[32] Periodic boundary condition is chosen here only for numerical purposes. It would not be deemed a good assumption if this model were about polarization between two extremes. However, this is not a critical issue because the objective of this study is to characterize not such polarization but disagreement between opinionated groups, and also even the concept of polarization itself can be much more nuanced than simple binary division [38, 39].

[33] Alan M Turing. The chemical basis of morphogenesis. *Philosophical Transactions of the Royal Society of London. Series B, Biological Sciences*, 237(641):37–72, 1952.

[34] John E Pearson. Complex patterns in a simple system. *Science*, 261(5118):189–192, 1993.

[35] Hiroki Sayama, Marcus AM de Aguiar, Yaneer Bar-Yam, and Michel Baranger. Spontaneous pattern formation and genetic invasion in locally mating and competing populations. *Physical Review E*, 65(5):051919, 2002.

[36] Shigeru Kondo and Takashi Miura. Reaction-diffusion model as a framework for understanding biological pattern formation. *Science*, 329(5999):1616–1620, 2010.

[37] Hiroki Sayama and Junichi Yamanoi. Beyond social fragmentation: Coexistence of cultural diversity and structural connectivity is possible with social constituent diversity. In *Proceedings of NetSci-X 2020: Sixth International Winter School and Conference on Network Science*, pages 171–181. Springer, 2020.

[38] Aaron Bramson, Patrick Grim, Daniel J Singer, Steven Fisher, William Berger, Graham Sack, and Carissa Flocken. Disambiguation of social polarization concepts and measures. *Journal of Mathematical Sociology*, 40(2):80–111, 2016.

[39] Aaron Bramson, Patrick Grim, Daniel J Singer, William J Berger, Graham Sack, Steven Fisher, Carissa Flocken, and Bennett Holman. Understanding polarization: Meanings, measures, and model evaluation. *Philosophy of Science*, 84(1):115–159, 2017.

Appendix A: Relationship between local and non-local gradients

Here we show that the non-local gradient $G(P)$ introduced in this study converges to a simple local gradient (derivative) P' in the limit of $\mu \to 0^+$ and $\sigma \to 0^+$, as follows:

$$\lim_{\mu,\sigma\to 0^+} G(P) = \lim_{\mu\to 0^+} \frac{1}{2\mu} \lim_{\sigma\to 0^+} \int_{-\infty}^{\infty} P(x+y) \cdot \frac{1}{\sqrt{2\pi}\sigma} \left(e^{-\frac{1}{2}\left(\frac{y-\mu}{\sigma}\right)^2} - e^{-\frac{1}{2}\left(\frac{y+\mu}{\sigma}\right)^2} \right) dy \tag{A1}$$

$$= \lim_{\mu\to 0^+} \frac{P(x+\mu) - P(x-\mu)}{2\mu} \tag{A2}$$

$$= P'(x) \tag{A3}$$

We also confirmed this convergence numerically (results not shown).

Appendix B: Details of linear stability analysis

We replace $P(x,t)$ in Eq. (1) with a homogeneous population level P_h plus a sinusoidal spatial perturbation with temporally changing small amplitude $\Delta P(t)$, as follows:

$$P(x,t) \to P_h + \Delta P(t) \sin(\omega x + \phi) \tag{B1}$$

Then Eq. (1) is rewritten as follows:

$$\sin(\omega x+\phi)\frac{d\Delta P}{dt} = -d\omega^2 \sin(\omega x+\phi)\Delta P - c\frac{\partial}{\partial x}\left[(P_h + \Delta P \sin(\omega x+\phi)) \int_{-\infty}^{\infty} (P_h + \Delta P \sin(\omega(x+y)+\phi))\, g(y) dy \right] \tag{B2}$$

By ignoring the second-order term of ΔP and exploiting the fact that $g(y)$ is an odd function, this equation is linearly approximated as follows:

$$\sin(\omega x+\phi)\frac{d\Delta P}{dt} \approx -d\omega^2\sin(\omega x+\phi)\Delta P - cP_h\frac{\partial}{\partial x}\int_{-\infty}^{\infty}\Delta P\sin(\omega(x+y)+\phi)g(y)dy \tag{B3}$$

$$= -d\omega^2\sin(\omega x+\phi)\Delta P - c\omega P_h\Delta P\int_{-\infty}^{\infty}\left[\cos(\omega x+\phi)\cos(\omega y)-\sin(\omega x+\phi)\sin(\omega y)\right]g(y)dy \tag{B4}$$

$$= -d\omega^2\sin(\omega x+\phi)\Delta P + c\omega P_h\sin(\omega x+\phi)\Delta P\int_{-\infty}^{\infty}\sin(\omega y)g(y)dy \tag{B5}$$

By dividing all terms by $\sin(\omega x+\phi)$ and collecting the coefficients of ΔP together, we obtain the following one-dimensional linear dynamical equation of ΔP:

$$\frac{d\Delta P}{dt} = \left(-d\omega^2 + c\omega P_h\int_{-\infty}^{\infty}\sin(\omega y)g(y)dy\right)\Delta P \tag{B6}$$

If the coefficient inside the parentheses above is positive, the small perturbation $\sin(\omega x+\phi)$ will grow, i.e., the homogeneous population distribution will be unstable and non-homogeneous patterns (distinct groups) will form.

With $Q(\omega) = \int_{-\infty}^{\infty}\frac{\sin(\omega y)}{\omega}g(y)dy$, this condition for pattern formation is summarized as

$$Q(\omega) > \frac{d}{cP_h} \tag{B7}$$

for $\omega > 0$, as described in the main text.

Appendix C: Properties of $Q(\omega)$

We note that $Q(\omega)$ is, by itself, the generalized nonlocal gradient of $\sin(\omega x)/\omega$ around $x = 0$. This indicates that the range of $Q(\omega)$ is bounded by the range of the gradients of the original function $\sin(\omega x)/\omega$, which is $\cos(\omega x)$, hence $Q(\omega) \in [-1, 1]$.

Moreover, we show that $Q(\omega)$ approaches its maximum 1 regardless of the shape of $g(y)$ in the limit of $\omega \to 0$, as follows:

$$\lim_{\omega\to 0} Q(\omega) = \lim_{\omega\to 0}\int_{-\infty}^{\infty}\frac{\sin(\omega y)}{\omega}g(y)dy \tag{C1}$$

$$= \lim_{\omega\to 0}\int_{-\infty}^{\infty} y\, g(y)dy \tag{C2}$$

$$= 1 \tag{C3}$$

Appendix D: Numerical simulations demonstrating the $cP_h > d$ instability condition

Our analysis shows that, if the opinion space is sufficiently large, the low-frequency perturbations always destabilize the homogeneous population distribution if and only if $cP_h > d$. This prediction can be confirmed through numerical simulations. Illustrative cases are shown in Fig. 6.

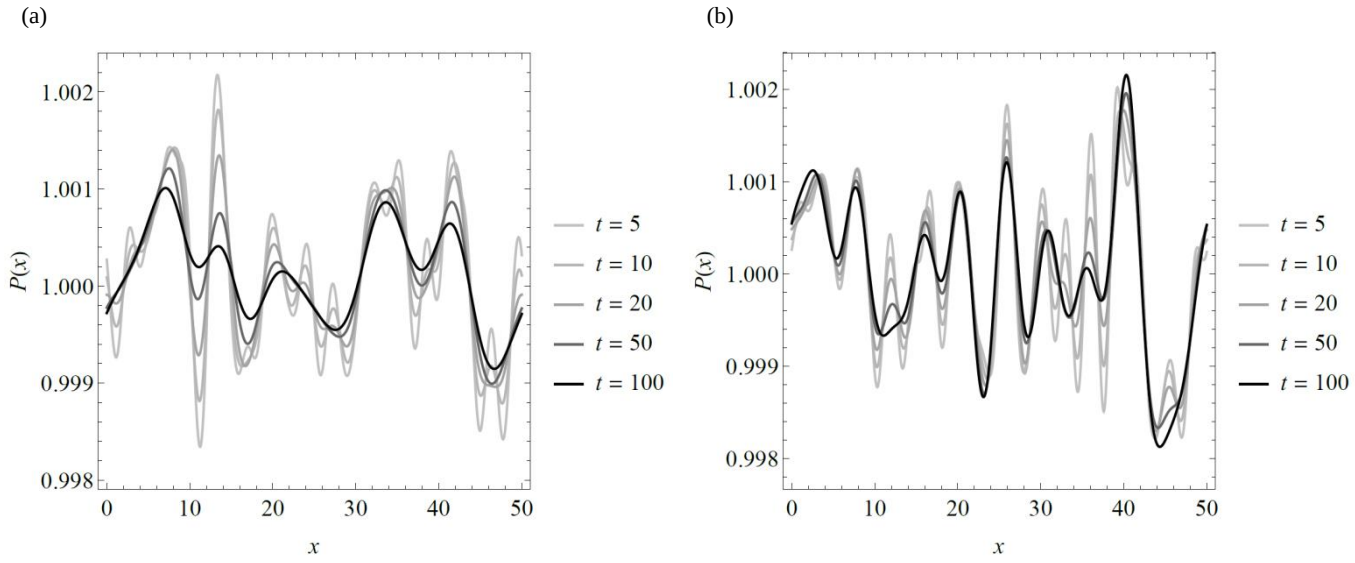


FIG. 6. Numerical simulation results with $c = P_h = 1$ and $\sigma = \mu = 0.1$. (a) Result with $d = 1.01$, which is slightly above $cP_h = 1$, therefore even the lowest-frequency perturbations gradually decay. (b) Result with $d = 0.99$, which is slightly below $cP_h = 1$, therefore lowest-frequency perturbations gradually grow and some peaks become more manifested over time. See the Methods section for details of numerical integration. Note that the vertical axis is set on a small range to show subtle difference between these two cases.